Brazilian Journal
of Chemical
Engineering

ISSN 0104-6632
Printed in Brazil
www.abeq.org.br/bjche

Vol. 29, No. 04, pp. 807 - 820, October - December, 2012

OPTIMIZATION AND CONTROL OF A CONTINUOUS POLYMERIZATION REACTOR

L. A. Alvarez* and D. Odloak

Department of Chemical Engineering, Polytechnic School, University of São Paulo,
Av. Prof. Luciano Gualberto, Trav. 3, 380, CEP: 05508-900, São Paulo - SP, Brazil.
Phone: + (55) (11) 30912237, Fax: + (55) (11) 38132380.
E-mail: luz@pqi.ep.usp.br; odloak@usp.br

(Submitted: May 27, 2011 ; Revised: December 9, 2011 ; Accepted: December 30, 2011)

Abstract - This work studies the optimization and control of a styrene polymerization reactor. The proposed strategy deals with the case where, because of market conditions and equipment deterioration, the optimal operating point of the continuous reactor is modified significantly along the operation time and the control system has to search for this optimum point, besides keeping the reactor system stable at any possible point. The approach considered here consists of three layers: the Real Time Optimization (RTO), the Model Predictive Control (MPC) and a Target Calculation (TC) that coordinates the communication between the two other layers and guarantees the stability of the whole structure. The proposed algorithm is simulated with the phenomenological model of a styrene polymerization reactor, which has been widely used as a benchmark for process control. The complete optimization structure for the styrene process including disturbances rejection is developed. The simulation results show the robustness of the proposed strategy and the capability to deal with disturbances while the economic objective is optimized.
Keywords: Polymerization reactor optimization; Model predictive control; Robust operation; Styrene reactor.

INTRODUCTION

The increasing necessity to optimize the operation of chemical reactors is related to the more competitive global market of chemical commodities and specialities. The more competitive a specific market, the more sophisticated the optimization and control strategies of the related industrial plant should be. In the industrial environment, the processes usually operate in a hierarchical structure, where the real time optimization (RTO) and the model predictive control (MPC) are executed in separated stages. The RTO routine determines the operating values of the outputs and inputs that produce the maximum economic profit or the lowest operating costs. In the context of the hierarchical structure, the objective of the MPC controller is to follow the economic targets in the presence of disturbances through the direct manipulation of the process inputs.

One of the main issues in the application of MPC to industrial processes, where real time optimization is present, is the stability of the closed loop system. Nominal stability is defined when there is not a mismatch between the model used in the controller and the real process model. Nominally stable MPCs can be found in the control literature since the seminal work of Muske and Rawlings (1993). However, when one deals with a structure where RTO is implemented, a nominally stable MPC is of little use. This is so because RTO is capable of changing the operating point of the process system quite significantly and the nominal model is no longer reliable. When one deals with process uncertainty, the guarantee of stability has to be extended in order to obtain a robust controller. In this work, an algorithm to integrate the RTO and the MPC is considered that assures stability for the whole hierarchical system when there is polytopic

*To whom correspondence should be addressed

uncertainty in the styrene reactor dynamic model. The MPC stage is based on an infinite horizon controller that includes a terminal state constraint (Odloak, 2004), which is extended to uncertain systems. Here, the zone control strategy is also considered (Gonzalez and Odloak, 2009), which consists of mantaining the process outputs inside allowed bounds instead of controlling the process at set-points. The optimization and control structure of the styrene polymerization reactor is tested for the case where the product viscosity and reactor temperature have to be regulated.

The optimization of polymerization processes has been the focus of several works (Kadam *et al*., 2007; Silva and Oliveira, 2002; Abel and Marquardt, 2003; Asteasuain and Brandolin, 2008). Some of them are dedicated to calculate optimal profiles to achieve the final desired properties in a minimum time. In other works, for example Kadam *et al*. (2007), the time for polymer grade transition is minimized in order to avoid a considerable amount of off-specification product. In this work, the continuous operation of a styrene polymerization reactor is optimized in a multilayer structure that includes: the RTO layer where an economic objective is considered subject to a rigorous nonlinear model of the polymerization reactor, a control layer where an MPC controller that is robust to a class of model uncertainty, and a target calculation stage that coordinates the communication between the two other layers such that the stability of the control structure is preserved.

In the next section, the styrene polymerization reactor is described; the phenomenological model is presented as well as the linear dynamic models that were obtained. Then, the robust algorithm that integrates the RTO and the MPC controller is presented. Then, the complete real time optimization of the styrene reactor is developed, showing the capability of the proposed strategy to optimize the polymerization process. Finally, in the last section the paper is concluded.

THE STYRENE POLYMERIZATION REACTOR

In this section, we present the main aspects of the reactor system that is studied here and that motivated the development of the control structure that allows the robust operation of the reactor.

Process Description

The polymerization reactor is usually the heart of the polymer production process and its operation may be difficult as it involves exothermic reactions, unknown reaction kinetics and high viscosity. Most styrene polymers are produced through batch or continuous polymerization processes. The present work considers the free-radical bulk and solution styrene polymerization in a jacketed CSTR. As shown in Fig. 1, the CSTR has three feed streams: the pure styrene monomer, the 2,2'-azoisobutyronitrile (AIBN) initiator dissolved in benzene, and the pure benzene solvent. The exit stream contains polymer, un-reacted monomer, initiator, and solvent. The kinetic mechanism used for this homopolymerization process is very general and can be described by the following steps (Jaisinghani and Ray, 1977):

$$I \xrightarrow{f_i, k_d} 2R \qquad \text{(initiator decomposition)}$$

$$M + R \xrightarrow{k_i} P_1 \qquad \text{(chain initiation)}$$

$$P_n + M \xrightarrow{k_p} P_{n+1} \qquad \text{(propagation)}$$

$$P_n + P_m \xrightarrow{k_{td}} T_n + T_m \qquad \text{(termination by disproportionation)}$$

$$P_n + P_m \xrightarrow{k_{tc}} T_{n+m} \qquad \text{(termination by combination)}$$

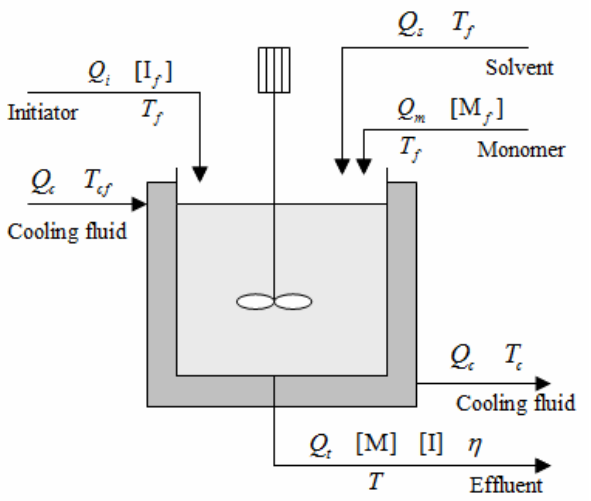

Figure 1: Process diagram for the styrene polymerization reactor

The two initiation reactions involve the decomposition of initiator I to produce radicals R, which react with the monomer molecules M to initiate new live (radical) polymer chains P_1. During the propagation step, monomer molecules M are added, one at a time, to the live-polymer chains

P_n ($n \geq 1$). The growth of the chains terminates when the propagating radicals lose their activity through any termination reaction, resulting in dead-polymer chains, T_n ($n \geq 1$).

Hidalgo and Brosilow (1990) and Maner *et al*. (1996) developed a phenomenological model for the styrene reactor. The following considerations lead to the phenomenological model given by Equations (1) to (10):

- The lifetime of the polymer radical species is extremely short compared to other system time constants. Then the quasi-steady-state approximation (QSSA) is considered for R and P_n;
- The monomer consumption is mainly due to propagation (Biensenberg and Sebastian, 1983), this leads to the Long Chain Assumption (LCA);
- Following Hidalgo and Brosilow (1990), the chain transfer reactions to monomer and to solvent are not considered;
- Monomer thermal initiation does not occur because this reaction is only significant at temperatures greater than 373K (Biensenberg and Sebastian, 1983). The reactor temperature considered in this work is below this limit;
- The overall chain termination rate constant, k_t, is composed of both combination, k_{tc}, and disproportionation, k_{td}, contributions (Schmidt and Ray, 1981) or $k_t = k_{tc} + k_{td}$. For styrene in solution, experimental results showed that the chain termination occurs solely by combination (Timm and Rachow, 1974). Then, termination by disproportionation is not considered, i.e. $k_t = k_{tc}$;
- According to the model presented in Maner *et al*. (1996), the rate of propagation is much faster than the rate of termination;
- The heats of initiation and termination are negligible compared to the heat of polymerization (Hidalgo and Brosilow, 1990).

The styrene reactor model is defined as follows:

$$\frac{d[I]}{dt} = \frac{(Q_i[I_f] - Q_t[I])}{V} - k_d[I] \tag{1}$$

$$\frac{d[M]}{dt} = \frac{(Q_m[M_f] - Q_t[M])}{V} - k_p[M][P] \tag{2}$$

$$\frac{dT}{dt} = \frac{Q_t(T_f - T)}{V} + \frac{(-\Delta H_r)}{\rho C_p} k_p[M][P] - \frac{hA}{\rho C_p V}(T - T_c) \tag{3}$$

$$\frac{dT_c}{dt} = \frac{Q_c(T_{cf} - T_c)}{V_c} + \frac{hA}{\rho_c C_{pc} V_c}(T - T_c) \tag{4}$$

where,

$$[P] = \left[\frac{2f_i k_d[I]}{k_t}\right]^{0,5} \tag{5}$$

$$k_j = A_j \exp\left(\frac{-E_j}{T}\right), \quad j = d, p, t \tag{6}$$

$$Q_t = Q_i + Q_s + Q_m \tag{7}$$

The definition of the parameters and variables involved in the equations above can be found in Tables 1 and 2, respectively. The moment equations for the dead polymer are written as follows:

$$\frac{dD_0}{dt} = 0,5k_t[P]^2 - \frac{Q_t D_0}{V} \tag{8}$$

$$\frac{dD_1}{dt} = M_m k_p[M][P] - \frac{Q_t D_1}{V} \tag{9}$$

$$\frac{dD_2}{dt} = 5M_M k_p[M][P] + 3M_M \frac{k_p{}^2}{k_t}[M]^2 - \frac{Q}{V} D_2 \tag{10}$$

D_0, D_1 and D_2 represent the zero, the first and the second order moment of the dead polymer, respectively.

The weight-average molecular weight is obtained as:

$$\overline{M}_w = M_m \frac{D_2}{D_1} \tag{11}$$

There are some vendors of instruments to measure efficiently molecular weights by gel permeation chromatography or size-exclusion chromatography, as reported by Richards and Congalidis (2006). However, for online control, it is more common to measure the viscosity as a substitute for the average molecular weights. In this work, it is assumed that an online viscosimeter provides reliable measurements of the intrinsic viscosity η. The following correlation is used to simulate the measurement of the viscosity (Gazi *et al*., 1996):

$$\eta = 0.0012(\overline{M}_w)^{0.71} \tag{12}$$

Table 1: Process parameters for the polymerization reactor

Variable	Symbol	Value	Units
Frequency factor for initiator decomposition	A_d	$2.142x10^{17}$	h^{-1}
Activation energy for initiator decomposition	E_d	14897	K
Frequency factor for propagation reaction	A_p	$3.816x10^{10}$	$L.mol^{-1}.h^{-1}$
Activation energy for propagation reaction	E_p	3557	K
Frequency factor for termination reaction	A_t	$4.50x10^{12}$	$L.mol^{-1}.h^{-1}$
Activation energy for termination reaction	E_t	843	K
Initiator efficiency	f_i	0,6	
Heat of polymerization	$-\Delta H_r$	$6.99 x10^{4}$	$J.mol^{-1}$
Overall heat transfer coefficient	hA	$1.05x10^{6}$	$J.K^{-1}.h^{-1}$
Mean heat capacity of reactor fluid	ρC_p	1506	$J.K^{-1}.L^{-1}$
Heat capacity of cooling jacket fluid	$\rho_c C_{pc}$	4043	$J.K^{-1}.L^{-1}$
Molecular weight of the monomer	M_m	104.14	$g.mol^{-1}$

Table 2: Steady-state operational condition for the polymerization reactor

Variable	Symbol	Value	Units
Flow rate of initiator	Q_i	108	$L.h^{-1}$
Flow rate of solvent	Q_s	459	$L.h^{-1}$
Flow rate of monomer	Q_m	378	$L.h^{-1}$
Flow rate of cooling jacket fluid	Q_c	471.6	$L.h^{-1}$
Reactor volume	V	3000	L
Volume of cooling jacket fluid	V_c	3312.4	L
Concentration of initiator in feed	$[I_f]$	0.5888	$mol.L^{-1}$
Concentration of monomer in feed	$[M_f]$	8.6981	$mol.L^{-1}$
Temperature of reactor feed	T_f	330	K
Inlet temperature of cooling jacket fluid	T_{cf}	295	K
Concentration of initiator in the reactor	[I]	$6.6832x10^{-2}$	$mol.L.^{-1}$
Concentration of monomer in the reactor	[M]	3.3245	$mol.L.^{-1}$
Temperature of the reactor	T	323.56	K
Temperature of cooling jacket fluid	T_c	305.17	K
Molar concentration of dead polymer chains	D_0	$2.7547x10^{-4}$	$mol.L^{-1}$
Mass concentration of dead polymer chains	D_1	16.110	$g.L^{-1}$

The polydispersity index (PD) is a property of the molecular weight distribution of the dead polymer, defined as:

$$PD = M_m \frac{D_2 D_0}{D_1^2} \quad (13)$$

The phenomenological model of this styrene reactor was first published in 1990 and, since then, it has been widely used as a benchmark for process control studies (Maner *et al*., 1996; Gazi *et al*., 1996; Kendi and Doyle, 1998; Prasad *et al*., 2002; Asteasuain *et al*., 2006; Sotomayor *et al*., 2007). Prasad *et al*. (2002) implemented a nonlinear MPC strategy for the control of the properties of the polymer. For optimal grade transition, Asteasuain *et al* (2006) developed a multi-objective optimization that focuses simultaneously on the process design and control parameters. In this work, the aim is to optimize on-line the production rate using a hierarchical structure. The real time optimization is developed in the upper stage and an intermediary routine recalculates the optimizing targets which are sent to the MPC controller. These stages are tied together and one needs to guarantee the stability of the complete control structure.

Control System and Prediction Models

The purpose of the control system of the styrene reactor is mainly to follow targets for outputs and inputs while mantaining the controlled outputs inside allowed zones. Here, the weight average molecular weight $\overline{M}_w$ and the reactor temperature T are defined as the controlled outputs. As on-line measurements of $\overline{M}_w$ are rarely available, the polymer intrinsic viscosity η is used instead. For controlling $y_1=\eta$ and $y_2=T$, the controller manipulates the initiator flowrate ($u_1= Q_i$) and the liquid flow rate of the cooling jacket ($u_2= Q_c$) because of the adequate sensitivity of the process outputs to these variables. The remaining inlet

flowrates Q_s and Q_m are related to Q_i by ratio control. So as to improve the performance of the controller, the ratio between the initiator flow rate Q_i and monomer flow rate Q_m is maintained fixed, then:

$$Q_m = \frac{\bar{Q}_m}{\bar{Q}_i} Q_i , \tag{14}$$

where $\bar{Q}_m$ and $\bar{Q}_i$ are the nominal values of Q_m and Q_i, respectively. On the other hand, the solvent volume fraction should be maintained at 0.6 to avoid the gel effect (Hidalgo and Brosilow, 1990), then a control law for the solvent flow rate is implemented as:

$$Q_s = 1.5Q_m - Q_i \tag{15}$$

The control structure considered for the styrene reactor requires linear models. These models were obtained empirically by step response tests. The nominal model, denoted as MN, used for prediction is the following transfer function model in the Laplace domain is:

$$G(s) = \begin{bmatrix} \dfrac{-66.69}{(1+5.3474s)(1+2.5274s)} & \dfrac{5.9425}{(1+7.6525s)(1+3.091s)(1+2.7063s)} \\ \dfrac{144.7925}{(1+6.7599s)(1+1.5797s)} & \dfrac{-47.5589}{(1+7.6173s)(1+2.3968s)} \end{bmatrix}$$

This model relates process inputs and outputs; it was obtained at the nominal operating point presented in the Table 2.

As the aim of this work is to develop an MPC controller that is capable of controlling styrene polymerization reactor at different operating points defined by the RTO stage, two additional models, each one corresponding to a different operating point around the nominal steady-state, were obtained. By modifying the values of the inputs u_1 and u_2, from the nominal values $\bar{u}_1$ and $\bar{u}_2$, new steady-states were obtained and the new linear dynamic models that represent the system around these steady states (Fig. 2) were included in the control problem formulation. The first additional model, denoted by M1, obtained at the steady-state defined by u_1=1.1 $\bar{u}_1$ and u_2=0.95 $\bar{u}_2$, is the following:

M1:

$$G(s) = \begin{bmatrix} \dfrac{-61.505}{(1+5.9946s)(1+2.3723s)} & \dfrac{6.9783}{(1+8.4587s)(1+2.9801s)(1+2.9801s)} \\ \dfrac{166.6494}{(1+7.542s)(1+1.501s)} & \dfrac{-59.0134}{(1+8.4433s)(1+2.5133s)} \end{bmatrix}$$

Analogously, for the steady-state defined through u_1=0.75 $\bar{u}_1$ and u_2=1.15 $\bar{u}_2$, it was obtained model M2 that is represented as follows:

M2:

$$G(s) = \begin{bmatrix} \dfrac{-90.853}{(1+6.6137s)(1+3.4171s)(1+3.3297s)} & \dfrac{4.2497}{(1+6.1175s)(1+3.2567s)(1+2.2792s)} \\ \dfrac{116.4704}{(1+5.6145s)(1+1.5327s)} & \dfrac{-29.3225}{(1+6.1047s)(1+2.152s)} \end{bmatrix}$$

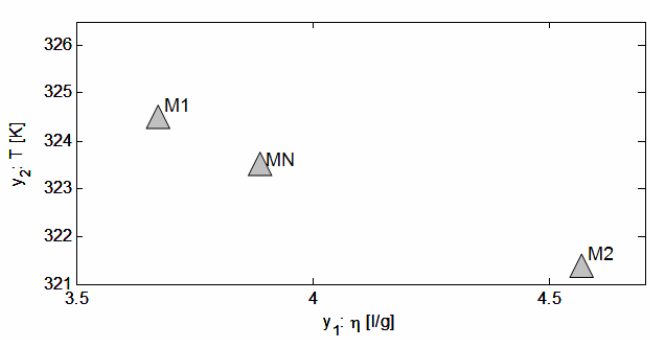

Figure 2: Steady-states values of T and η where the linear models MN, M1 and M2 were obtained.

It is clear that the models defined above do not have the same gain or the same time constants as the nominal model. Then the effect on the output prediction is significant. So, there is motivation to consider a control structure where stability and performance is preserved despite the operation at quite different steady-states.

ROBUST CONTROL STRATEGY

The rigorous steady-state version of the model defined through Equations (1) to (13) is used to represent the true reactor at steady-state in the optimization problem that defines the RTO stage of the structure represented in Fig. 3. The MPC stage is based on a robust linear MPC that is presented next.

System Representation

Although the available dynamic models of the styrene reactor are in the transfer function form, the MPC considered here is based on a state space model as is usual in modern MPC packages. To describe this model, let us consider a system with nu inputs and ny outputs, and assume that the poles that relate the input u_i to the output y_j are non-repeated. A state space model that is suitable to the implementation of an offset free MPC can be represented in the following form (Odloak, 2004):

$$\begin{bmatrix} x^s(k+1) \\ x^d(k+1) \end{bmatrix} = \begin{bmatrix} I_{ny} & 0 \\ 0 & F \end{bmatrix} \begin{bmatrix} x^s(k) \\ x^d(k) \end{bmatrix} + \begin{bmatrix} D^0 \\ D^d \end{bmatrix} \Delta u(k) \quad (16)$$

$$y(k) = \begin{bmatrix} I_{ny} & \Psi \end{bmatrix} \begin{bmatrix} x^s(k) \\ x^d(k) \end{bmatrix}$$

where

$$x^s = \begin{bmatrix} x_1 & \cdots & x_{ny} \end{bmatrix}^T,\ x^s \in \mathbb{R}^{ny},$$

$$x^d = \begin{bmatrix} x_{ny+1} & x_{ny+2} & \cdots & x_{ny+nd} \end{bmatrix}^T,\ x^d \in \mathbb{C}^{nd},$$

$$F \in \mathbb{C}^{nd.nd},\ \Delta u(k) = u(k) - u(k-1),\ \Psi \in \mathbb{R}^{ny \times nd}$$

The input in the model defined in Eq. (16) is $\Delta u(k)$, which means that the output integrates the input. In this model, the state vector is split in two parts: x^s that corresponds to the integrating poles produced by the incremental form of the model, and x^d that corresponds to the system modes. The state component x^s corresponds to $y(\infty|k)$ that is the predicted output at steady-state. For stable systems, it is easy to show that when the system approaches the steady-state, component x^d tends to zero. F is a diagonal matrix with components corresponding to the poles of the system. The system has nd stable poles.

In the model defined in Eq. (16), model uncertainty is related to the uncertainty in matrices F, D^0 and D^d, as discussed in Alvarez and Odloak (2010). Then, suppose one defines the set of possible plants as $\Omega = \{\theta_1, \theta_2, ...\theta_L\}$, where each θ_i corresponds to a particular plant $\theta_i = \left(F_i, D_i^0, D_i^d\right)$, $i = 1,2,...L$. The true model of the process system is unknown, but one can assume that it can be represented as $\theta_r = \left(F_r, D_r^0, D_r^d\right)$, where $\left(D_r^0, D_r^d\right) = \sum_{i=1}^{L} \lambda_i \left(D_i^0, D_i^d\right)$, $\sum_{i=1}^{L} \lambda_i = 1,\ \lambda_i \geq 0$ and $F_r = F_{j=1,2...L}$. This means that the pair of matrices

D_r^0 and D_r^d lies in a convex polytope defined by L vertices (Kothare *et al*., 1996), while F_r belongs to a finite set of possible dynamics (Badgwell, 1997). In this way, uncertainty in the gain matrices D_r^0, D_r^d is defined as polytopic (Kothare *et al*., 1996) while the uncertainty in F is assumed to be of the multi-plant type (Badgwell, 1997). Assume also that there is a most likely plant that also lies in Ω and is denoted by θ_n.

Badgwell (1997) developed a robust linear quadratic regulator for stable systems with the multi-plant uncertainty. Later, Odloak (2004) extended the method of Badgwell to the output tracking of stable systems considering the same kind of model uncertainty. These strategies include a constraint to each of the models lying in Ω that prevents the increase of the true plant cost function at sucessive time steps. Gonzalez and Odloak (2009) proposed a stable MPC controller where the outputs are controlled by zones instead of at fixed set-points. In the method followed here, the approach of Odloak (2004) and the zone control strategy are applied to the multiple stage structure represented in Fig. 3, as described in the following section.

Control Structure

The control structure considered in this work is represented in Fig. 3. In this structure, the RTO layer is dedicated to the calculation of the desired targets u_{RTO} and y_{RTO}, for the input and output variables of the styrene reactor. This layer is commonly based on the rigorous stationary model and takes into account the process measurements and the economic parameters. The second layer is the target calculation (TC) algorithm that, at each time step, re-computes feasible steady-state operating points assuming that the RTO routine produces piecewise constant optimizing references for inputs and outputs. As discussed in Ying and Joseph (1999), the main purpose of the target calculation routine is to compute achievable set-points for the MPC controller. The targets $y_{ref}^{\theta_i}(k)$, $i = 1,...L$ and $u_{ref}(k)$ are obtained through the solution of an optimization problem based on the nominal linear static model of the process system. Then, the solution of the TC stage is sent to the MPC controller, which is devoted to guide some of the reactor inputs and/or outputs to the desired values given by the TC stage, while keeping the other reactor controlled outputs within specified zones.

In terms of the frequency at which each stage is computed, the RTO stage is solved at a much slower pace than the lower level control stages. This allows a dynamic decoupling between the RTO stage and the TC/MPC stages. Thus, one observes that the stability of the styrene reactor in closed loop with the structure represented in Fig. 3 depends only on the interaction between the TC and MPC stages. Consequently, the target calculation stage, that coordinates the interaction between the RTO and MPC stages, has to be designed in such a way that stability of the control structure is preserved.

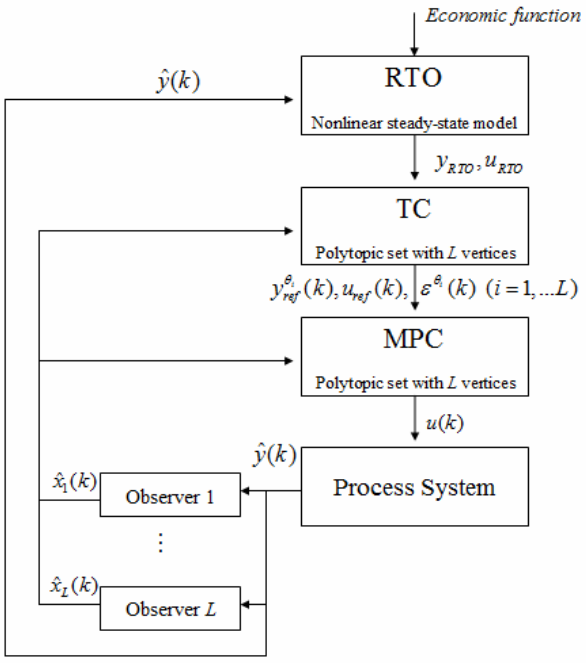

Figure 3: Styrene polymerization reactor control structure with RTO and MPC

On the other hand, note that from the control structure depicted in Fig. 3, there is one state observer per each model, and the observer corresponding to the true model θ_r is based on the true model matrices and will indicate the true state for the undisturbed system. In this case, at each sampling step, the corrected state is sent to the TC and MPC stages to calculate the next control action according to the algorithm that is described in the following section.

RTO Problem

The RTO layer deals with the economic optimization. In this case, the maximization of the production rate is considered as the economic objective. The production rate is defined as the product of the total flowrate Q_t and the first order moment D_1, this product represents the total weight of dead polymer produced per time unit. The RTO routine solves the following economic optimization problem:

$$\max_{y_{RTO},u_{RTO},x} \quad Q_t D_1 \tag{17}$$

subject to:

$$h(y_{RTO},u_{RTO},x)=0 \tag{18}$$

$$1.49 \le PD \le 1.51 \tag{19}$$

$$u_{min} \le u_{RTO} \le u_{max} \tag{20}$$

$$y_{min} \le y_{RTO} \le y_{max} \tag{21}$$

where,

$h(y_{RTO},u_{RTO},x)$ represents the nonlinear steady-state model and x is the vector of states of the phenomenological model, $x=\left[[I],[M],T,T_c,D_0,D_1,D_2\right]^T$. Observe that D_1 is one of the states of the phenomenological model in Eq. (8). The problem includes a bound constraint on the polydispersity PD, which depends on three states of the process model. This property is a strong indicator of the polymer quality. In this case, it is desired to maintain the polydispersity around the nominal value of 1.5. Note that this RTO problem is a nonlinear programming (NLP) since the constraints in Eqs. (18) and (19) are nonlinear. Here, it is assumed that the disturbances are measured and the optimization problem is updated at each sample time; both the process model state D_1 in Eq. (17) and the model constraints in Eqs. (18) and (19) are then modified as the disturbances are introduced. From the solution of this problem, only y_{RTO} and u_{RTO} are passed to the TC stage.

Robust Algorithm for the TC and MPC Stages

In this section, the robust structure, which is defined by the TC and the MPC optimization algorithms, is described. Let us denote the cost function for the TC stage at time k by J_k^{TC}. For each model i, $i=1,...L$ the objective function associated with model i is defined as follows:

$$J_k^{TC}(\theta_i)=\left\|y_{ref}^{\theta_i}(k)-y_{RTO}\right\|_{W_y}^2 + \left\|u_{ref}(k)-u_{RTO}\right\|_{W_u}^2+\left\|\varepsilon^{\theta_i}(k)\right\|_{S_i}^2 \tag{22}$$

where the weighting matrices W_y, W_u and S_i $(i=1...L)$ are positive definite.

Then, at the TC stage, the following optimization problem is solved (Alvarez and Odloak, 2010):

$$\min_{\substack{y_{ref}^{\theta_i}(k),u_{ref}(k),\varepsilon^{\theta_i}(k)\\ i=1,...L}} J_k^{TC}(\theta_n)+\sum_{\substack{i=1\\ i\neq n}}^{L}\left\|\varepsilon^{\theta_i}(k)\right\|_{S_i}^2$$

subject to:

$$u_{ref}(k)\in U,$$

$$U=\left\{u_{ref}(k)\left|\begin{array}{l}-m\Delta u_{max}\le u_{ref}(k)-u(k-1)\le m\Delta u_{max}\\ u_{min}\le u_{ref}(k)\le u_{max}\end{array}\right.\right\} \tag{23}$$

$$y_{ref}^{\theta_i}(k)-x^s(k)=D^0(\theta_i)\left[u_{ref}(k)-u(k-1)\right], \quad i=1,...L \tag{24}$$

$$y_{min}+\varepsilon^{\theta_i}(k)\le y_{ref}^{\theta_i}(k)\le y_{max}+\varepsilon^{\theta_i}(k), \quad i=1,...L \tag{25}$$

$$J_k^{TC}(\theta_i)\le \tilde{J}_k^{TC}(\theta_i), \qquad i=1,...L \tag{26}$$

In this problem, $\tilde{J}_k^{TC}(\theta_i)$ is the cost associated with the solution of the same problem at the previous sampling step that is defined as $\left\{\tilde{y}_{ref}^{\theta_i}(k),u_{ref}^*(k-1),\varepsilon^{\theta_i *}(k-1)\right\}$, where $\tilde{y}_{ref}^{\theta_i}(k)$ is such that:

$$\tilde{y}_{ref}^{\theta_i}(k) - x^s(k) + D^0(\theta_i)\Delta u(k-1) = D^0(\theta_i)\left(u_{ref}^*(k-1) - u(k-2)\right) \quad (27)$$

The TC optimization problem minimizes the cost for the nominal model θ_n subject to constraints related to models $\theta_1,...\theta_L$. The equality constraints Eq. (24) correspond to the steady-state linear models relating the predicted output with the desired steady-state, $u(k-1)$ is the control action applied to the real system at the previous time step, $\varepsilon^{\theta_i}(k)$ are slack variables that soften the bound constraints associated with each $y_{ref}^{\theta_i}(k)$ and allow these variables to take values outside the output control zone, and m is the control horizon of the MPC controller considered in the MPC stage in Fig. 3 The constraints represented in Eq. (24) force the decrease of the cost function J_k^{TC} for all the L models. Note that, if at time step k a disturbance enters the system the solution $\left\{y_{ref}^{\theta_i *}(k-1), u_{ref}^*(k-1), \varepsilon^{\theta_i *}(k-1)\right\}$ that is inherited from time $k-1$ may be unfeasible. By replacing $y_{ref}^{\theta_i *}(k-1)$ with $\tilde{y}_{ref}^{\theta_i}(k)$ computed through Equation (27), where the actual state $x^s(k)$ is used, the optimization problem of the TC stage is always feasible.

The optimal solution of the TC stage $\left\{y_{ref}^{\theta_i *}(k), u_{ref}^*(k), \varepsilon^{\theta_i *}(k)\right\}$ is then sent to the MPC stage, where a constrained infinite horizon MPC controller is implemented. The optimization problem, which has the same sampling period as the TC stage, is defined as follows:

$$\min_{\substack{\Delta u_k, y_{sp}^{\theta_i}(k), \delta^{\theta_i}(k) \\ i=1,...L}} J_k^{MPC}(\theta_n) + \sum_{\substack{i=1 \\ i\neq n}}^{L} \left\| \delta^{\theta_i}(k) \right\|_{P_i}^2$$

subject to:

$$\Delta u(k+j|k) \in V,$$

$$V = \left\{ \Delta u(k+j) \left| \begin{array}{l} -\Delta u_{max} \le \Delta u(k+j) \le \Delta u_{max} \\ u_{min} \le u(k-1) \\ + \sum_{i=0}^{j} \Delta u(k+i) \le u_{max} \\ \Delta u(k+j) = 0, \ j \ge m \end{array} \right. \right\} \quad (28)$$

$$x^s(k) + \tilde{D}^0(\theta_i)\Delta u_k - y_{sp}^{\theta_i}(k) - \delta^{\theta_i}(k) = 0, \quad i = 1,...L \quad (29)$$

$$\tilde{D}^0 = \underbrace{\left[D^0 \quad ... \quad D^0 \right]}_{m}$$

$$y_{sp}^{\theta_i}(k) = y_{ref}^{\theta_i *}(k) - \delta^{\theta_i}(k), \quad i = 1,...L \quad (30)$$

$$\delta^{\theta_i}(k) = \varepsilon^{\theta_i *}(k), \quad i = 1,...L \quad (31)$$

$$y_{min} \le y_{sp}^{\theta_i}(k) \le y_{max}, \quad i = 1,...L \quad (32)$$

$$u(k-1) + \tilde{I}\Delta u_k - u_{ref}^*(k) = 0 \quad (33)$$

$\tilde{I} = \underbrace{\left[I_{nu} \quad ... \quad I_{nu} \right]}_{m}$, I_{nu} is the identity matrix with dimension nu

$$J_k^{MPC}(\theta_i) \le \tilde{J}_k^{MPC}(\theta_i), \quad i = 1,...L \quad (34)$$

In this problem, the infinite horizon cost $J_k^{MPC}(\theta_i)$ is defined as:

$$J_k^{MPC}(\theta_i) = \sum_{j=0}^{\infty} \left[\begin{array}{l} \left\| \hat{y}^{\theta_i}(k+j|k) - y_{sp}^{\theta_i}(k) - \delta^{\theta_i}(k) \right\|_{Q_y}^2 \\ + \left\| u(k+j|k) - u_{ref}^*(k) \right\|_{Q_u}^2 \\ + \left\| \Delta u(k+j|k) \right\|_R^2 \end{array} \right] + \left\| \delta^{\theta_i}(k) \right\|_{P_i}^2 \quad (35)$$

$i = 1,...L$

where the weight matrices Q_y, Q_u, R and P_i $(i = 1...L)$ are positive definite.

The MPC controller resulting from the solution to the problem defined above and adopted to the control of the styrene reactor is based on the controller developed by Gonzalez and Odloak (2009) that is capable of dealing with input targets provided by the RTO and controlling the outputs inside zones. This controller also guarantees robust stability of the closed-loop system. In the problem of the MPC stage, $\delta^{\theta_i}(k)$ are the slack variables that guarantee

that the terminal constraints in Eq. (29) are always feasible and the cost functions $J_k^{MPC}(\theta_i),\ i=1,...L$ are bounded. Constraints in Eqs. (30) and (31) are applied only to those outputs that have optimizing targets, while constraint in Eq. (32) is written for the outputs without optimizing targets. Also, the equality of the slacks of the TC and MPC stage defined in Eq. (31) guarantee that the solution of the MPC problem will not disrupt the convergence of the cost function of the TC stage. The set of constraints in Eqs. (25) to (27) assures that the solution of the MPC problem is consistent with the solution of the TC stage problem. Constraint in Eq. (33) is related to the input targets, so it is only written for those inputs that have optimizing targets. The constraint represented in Eq. (34) involves the cost $\tilde{J}_k^{MPC}(\theta_i)$, which is calculated with the solution $\left\{\Delta\tilde{u}_k, \tilde{y}_{sp}^{\theta_i}(k), \tilde{\delta}^{\theta_i}(k)\right\}$, where:

$$\Delta\tilde{u}_k = \left[\ \Delta u^*(k|k-1)^T \ \ ... \ \ \Delta u^*(k+m-2|k-1)^T \ \ 0\ \right]^T$$

$$\tilde{y}_{sp}^{\theta_i}(k) = y_{sp}^{\theta_i *}(k-1), \qquad i=1,...L$$

and $\tilde{\delta}_{y,i}(k)$ is such that

$$x^s(k) + \tilde{D}^0(\theta_i)\Delta\tilde{u}_k - \tilde{y}_{sp}^{\theta_i}(k) - \tilde{\delta}_{sp}^{\theta_i}(k) = 0, \qquad i=1,...L$$

Observe that the set $\left\{\Delta\tilde{u}_k, \tilde{y}_{sp}^{\theta_i}(k), \tilde{\delta}^{\theta_i}(k)\right\}$ is a feasible solution inherited from the time instant $k-1$ based on the present state $x^s(k)$.

This control structure guarantees robust stability (Alvarez and Odloak, 2010). If the RTO targets are reachable, the process variables converge to the desired targets while the cost functions corresponding to the TC and MPC stages converge to zero for each model i (i=1,…L) and consequently for the true model. Otherwise, the cost function of the TC stage converges to a point where the distance between $\left(y_{RTO}, u_{RTO}\right)$ and $\left(y_{ref}^{\theta_n}, u_{ref}^{\theta_n}\right)$ is minimized.

In the next section, the behavior of this robust structure applied to the styrene polymerization reactor is tested.

SIMULATION RESULTS

For this simulation, targets for the output y_2 and input u_1 were defined. Two disturbances affect the process during 400 hours of simulation. This controller considers the three linear models for prediction. The simulation conditions are the following: The constraint values: u_{max} = [0.070 ; 0.25] ; u_{min} = [0.015 ; 0.08] ; Δu_{max} = [0.1 ; 0.1]; y_{max} = [4.15 ; 326] ; y_{min} = [3.5 ; 321]. The initial conditions: u_0 = [0.03; 0.131] ; y_0 = [3.9;323.5]. The following tuning parameters are considered: C_y = [0 1] ; C_u = [5 0] ; C_ε = 1e5×[1 1]; m = 3; Q_y = [1 1] ; Q_u = [200 0] ; R = [10 10] ; S_y = 1e5×[1 1].

First, at t=0 the process starts at a non-optimal steady-state and the controller tries to bring the process to the optimal target calculated by the RTO routine. Fig. 4 shows the process outputs (black line), RTO targets (green discontinuous line) and the targets calculated in the TC stage (blue discontinuous line). The output target for y_2 and output y_2 both reach the RTO target, which is at the upper bound of the zone, while output y_1 reaches a different steady-state value inside its control zone. As can be seen in Fig. 5, the input u_1 also reaches the RTO target. By observing Fig. 7, one can see that the production rate is increased and so the complete structure is efficient enough to maximize the production. Fig. 6 shows that, at the beginning, the cost function of the TC stage converges to zero and then in the MPC stage also converges, which means that the process variables followed the desired objectives.

The first disturbance occurs at time t=110h, and corresponds to a sudden decrease of 4 °C in the temperature of the feed. This disturbance has a large effect on y_1, which is the viscosity of the product and also, as expected, on y_2, the reactor temperature. Notice that both outputs are pushed to outside their zones and the control system brings them back to inside the zones. This disturbance moves the optimal steady-state and the RTO calculates new target values for both y_2 and u_1. Figure 4 shows that the new target for the output y_2 corresponds to a lower temperature and the control system is able to bring this output to its target. As can be seen in Fig. 5, the RTO sends a new target for u_1 which is easily reached, while the input u_2 decreases. This means that the flow rate of cooling fluid decreases to reduce the reactor temperature, according to the RTO target. The cost functions depicted in Fig. 6 show that the cost functions of both TC and MPC stages were affected and that the convergence of the MPC stage is only reached after the TC stage has converged. It is also interesting to observe in Fig. 7 that the production rate decreased suddenly due to the disturbance, but then increases reaching a new maximum value.

After 250 hours of simulation, when the process had reached the steady-state, a second disturbance was introduced in the reactor. There was an abrupt decrease from 0.59 to 0.54 mol/l in the initiator feed concentration. In this case, the RTO computes a different value for the targets of u_1 and y_2, both variables are able to reach the targets. Fig. 4 shows that this disturbance pushed the viscosity (y_1) to outside the zone and the TC target for y_1 decreases to the lower bound of the zone, then this target increases while the viscosity is recovered reaching the target. Note that at first, the controller was bringing the TC targets to a smaller value of y_1 and a larger value of u_2 to adjust the process to the new RTO targets. However, when the target for y_1 reached its lower bound, the controller had to readjust these TC targets to feasible values changing the direction of u_2. In this case, the process is moved to a new optimal steady-state, as shown in Fig. 5. This disturbance drives the process to an optimal production rate, which is larger than the last one, as can be seen in Fig. 7.

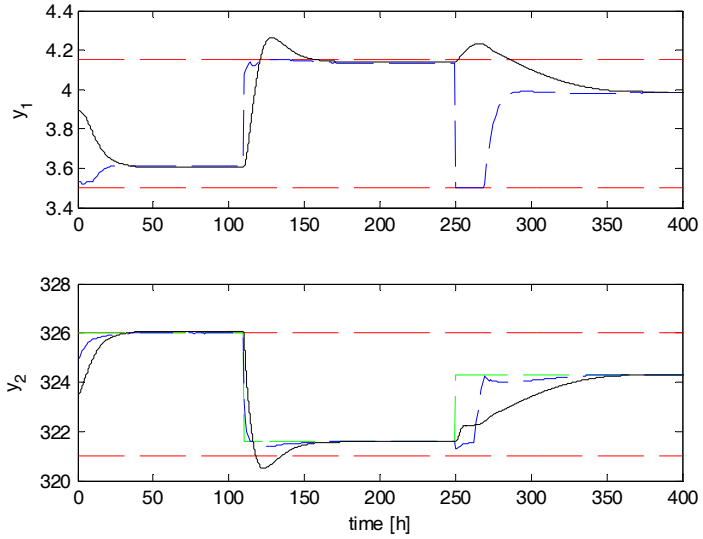

Figure 4: Process outputs. Red dashed line: Output bounds. Blue dashed line: calculated targets. Green dashed line: RTO targets. Solid line: Process outputs.

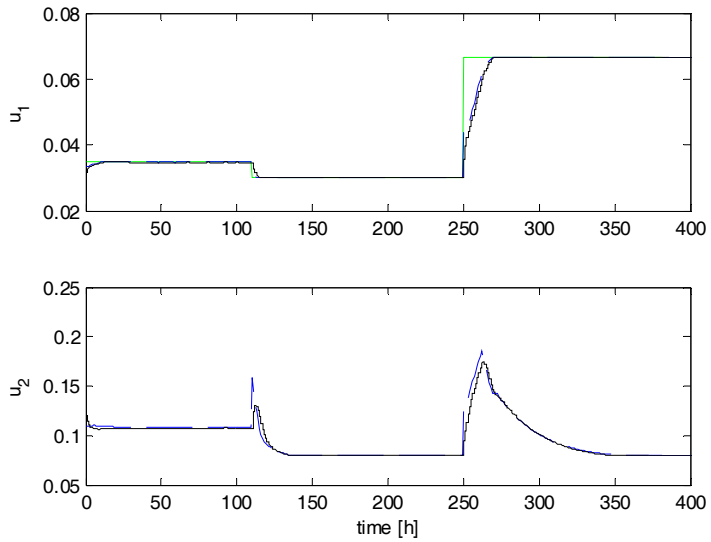

Figure 5: Process inputs. Blue dashed line: calculated input targets. Green dashed line: RTO input targets. Solid line: Process inputs.

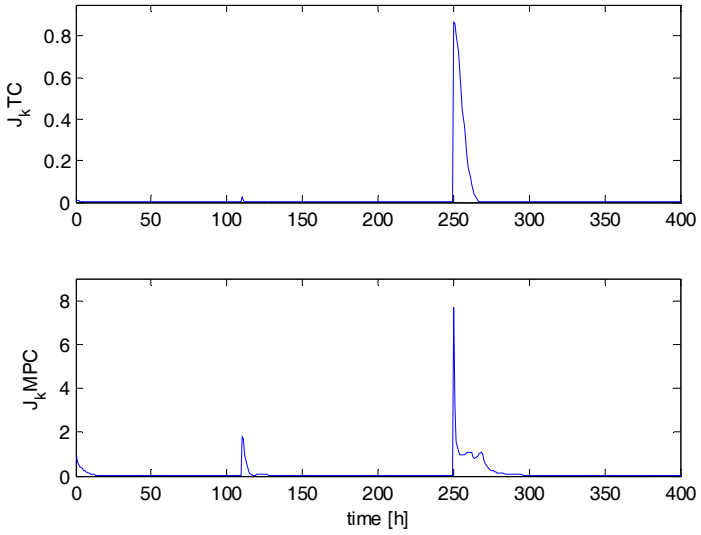

Figure 6: Cost functions of the robust control structure.

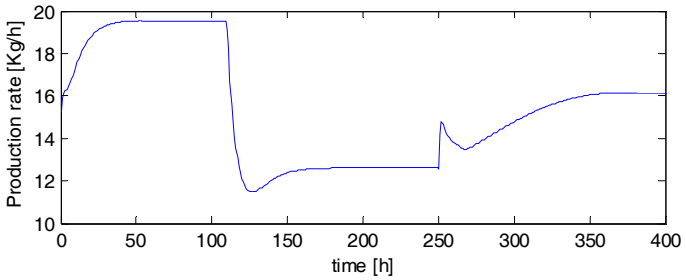

Figure 7: Production rate of the process.

The polydispersity is a property that indicates the distribution of the polymer chain size in the product. Additionally, the intrinsic viscosity η measures indirectly the average molecular weight of the polymer produced (Gazi *et al.*, 1996). Both molecular weight and polydispersity are strong indicators of polymer quality. Fig. 8 shows the simulation results for the polydispersity, it can be seen that this property remains near its nominal value of 1.5, respecting the limits imposed by the RTO problem even when disturbances affect the process.

Finally, Fig. 9 shows the optimal steady-states reached during the RTO simulation as a function of the outputs. The first steady-state (ON) corresponds to the optimal nominal conditions and, although it is close to the M1 steady-state, it is far from the remaining MN and M2 steady-states. The first disturbance brought the process to the optimal steady-state OD1, which is near the MN and M2. Then, the second disturbance moved the optimal steady-state to a point denoted by OD2, for this point, the MN is the closest steady-state. This demonstrates that the proposed robust RTO/TC/MPC strategy can deal with disturbances that drive the process to different operating points and result in different optimum points.

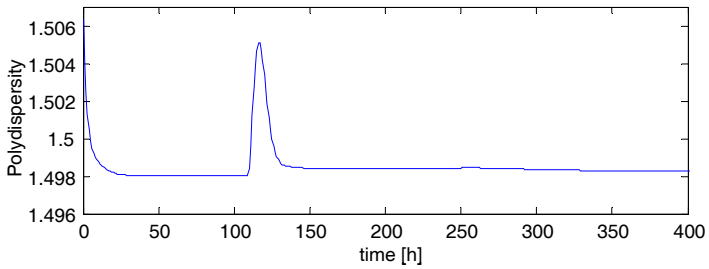

Figure 8: Polydispersity of the produced polymer

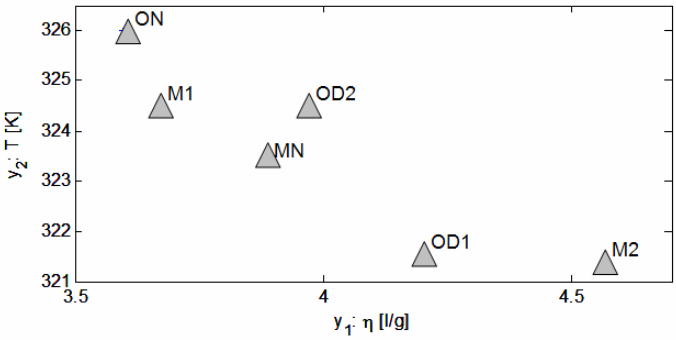

Figure 9: Steady-states values of T and η corresponding to the optimum at the nominal operating condition (ON), after the first disturbance (OD1), after the second disturbance (OD2) and where linear models MN, M1 and M2 were obtained

CONCLUSIONS

In this work the robust control and optimization of a styrene polymerization reactor was studied. The control structure includes a TC stage between the RTO and MPC routines which recalculates feasible targets for the MPC. Model uncertainty is considered in the TC and MPC stages of the control structure. For linear systems, the strategy assures stability in a polytopic region where the model uncertainty was defined. The resultant scheme is robust as the algorithm guarantees convergence to the desired targets for the uncertain model. The approach was simulated in the styrene polymerization reactor, which is a nonlinear system. Multiple linear dynamic models were obtained around different operating points, and considered as the vertices of a polytopic region where the real system operates. The simulation results of the complete RTO structure showed that the approach is capable of maximizing the production rate in the presence of disturbances, preserving the polymer quality and satisfying the allowed limits for the controlled outputs.

ACKNOWLEDGEMENTS

Authors are grateful to FAPESP for the financial support under grant 2008/57511-9.

REFERENCES

Abel, O. and Marquardt, W., Scenario-integrated on-line optimisation of batch reactors. J. Proc. Cont., 13, p. 703-715 (2003).

Alvarez, L. and Odloak, D., Robust integration of real time optimization with linear model predictive control. Comp. Chem. Eng., 34, p. 1937-1944 (2010).

Asteasuain, M., Bandoni, A., Sarmoria, C., Brandolin, A., Simultaneous process and control system design for grade transition in styrene polymerize-tion. Chem. Eng. Sci., 61, p. 3362-3378 (2006).

Asteasuain, M. and Brandolin, A., Modeling and optimization of a high-pressure ethylene polymerization reactor using gPROMS. Comp. Chem. Eng., 32, p. 396-408 (2008).

Badgwell, T., Robust model predictive control of stable linear systems. Int. J. Control, 68 (4), p. 797-818 (1997).

Biensenberg, J. and Sebastian, D., Principles of Polymerization Engineering. Wiley, New York (1983).

Gazi, E., Seider, W., Ungar, L., Verification of controllers in the presence of uncertainty: Application to styrene polymerization. Ind. Eng. Chem. Res., 35, p. 2277-2287 (1996).

González, A., Marchetti, J., Odloak, D., Extended robust model predictive control of integrating systems. AIChE J., 53, (7), p. 1758-1769 (2007).

González, A., Odloak, D., A stable model predictive control with zone control. J. Proc. Cont., 19, p. 110-122 (2009).

Hidalgo, P., Brosilow, C., Nonlinear model predictive control of styrene polymerization at unstable operating points. Comp. Chem. Eng., 14, p. 481-494 (1990).

Jaisinghani, R., Ray, W., On the dynamic behavior of a class of homogeneous continuous stirred tank polymerization reactor. Chem. Eng. Sci., 32, p. 811-825 (1977).

Kadam, J., Marquardt, W., Srinivasan, B. and Bonvin, D., Optimal grade transition in industrial polymerization processes via NCO tracking. AIChE J., 53, p. 627-639 (2007).

Kendi, T., Doyle III, F., Nonlinear internal model control for systems with measured disturbances and input constraints. Ind. Eng. Chem. Res., 37, p. 489-505 (1998).

Kothare, M., Balakrishnan, V., Morari, M., Robust constrained model predictive control using linear matrix inequalities. Automatica, 32, (80), p. 1361-1379 (1996).

Maner, B., Doyle III, F., Ogunnaike, B., Pearson, R., Nonlinear model predictive control of a simulated multivariable polymerization reactor using second-order Volterra models. Automatica, 32, (9), p. 1285-1301 (1996).

Odloak, D., Extended robust model predictive control. AIChE J., 50 (8), p. 1824-1836 (2004).

Prasad, V., Schley, M., Russo, L., Bequette, B., Product property and production rate control of styrene polymerization. J. Process Control, 12, p. 353-372 (2002).

Richards, J. and Congalidis, J., Measurement and control of polymerization reactors. Comp. Chem. Eng., 30, p. 1447-1463 (2006).

Schmidt, A. and Ray, W., The dynamic behavior of continuous polymerization reactors–I Isothermal solution polymerization in a CSTR. Chem. Eng. Sci., 36, p. 1401-1410 (1981).

Silva, D. and Oliveira, N., Optimization and nonlinear model predictive control of batch polymerization systems. Comp. Chem. Eng., 26, p. 649-658 (2002).

Sotomayor, O., Odloak, D., Giudici, R., Diagnosis of abnormal situations in a continuous solution polymerization reactor. Macromol. Theory Simul., 16, p. 247-261 (2007).

Timm, D. and Rachow, J., Description of polymerization dynamics by using population density. H. M., Hulburt, Chemical Reaction Engineering–II, Advances in Chemistry Series 133. Am. Chem. Soc., p. 122-136 (1974).

Ying, C., Joseph, B., Performance and stability analysis of LP-MPC and QP-MPC cascade control systems. AIChE J., 45, p. 1521-1534 (1999).